ASME Journal of Engineering for Gas Turbines and Power
Online journal at:
https://asmedigitalcollection.asme.org/gasturbinespower

A Comparative Study of Component Surrogate Model Approximation for Holistic, Multidisciplinary Optimization of High Temperature Heat Pumps

Jens Gollasch[1]
German Aerospace Center (DLR),
Institute of Low-Carbon Industrial Processes,
Cottbus 03046, Germany
e-mail: jens.gollasch@dlr.de

Michael Lockan
German Aerospace Center (DLR),
Institute of Low-Carbon Industrial Processes,
Cottbus 03046, Germany
e-mail: michael.lockan@dlr.de

Fast and reliable design methods are essential to reach the highest possible efficiency of high-temperature heat pumps and enable their full potential. The heat pump's performance is strongly dependent on the efficiency of its components like turbomachines and heat exchangers (HEX). Conventional design is a sequential procedure starting with the cycle conceptualization. Component performance is initially based on assumptions, and its design is optimized in subsequent steps with an increasing level of detail. This sequential aspect makes it impossible to find the overall optimal heat pump configuration. To overcome this, holistic design strategies optimize the cycle parameters simultaneously with detailed geometric component design. This concept leads to significantly improved heat pump performance, saves time and reduces uncertainty. Multidisciplinary optimizations are complex problems with a high number of design variables. This paper addresses two aspects of holistic heat pump design: A collaborative design architecture is introduced as a multilevel approach. Multiple components are designed in subproblems, which leads to a high number of required simulations. To mitigate high computational effort, the second focus is on the approximation of the component analyses with the use of computationally inexpensive surrogate models. It is found that Gaussian process regression is most accurate and outperforms both linear regression and radial basis functions (RBF). In comparison to previous studies, the number of iterations for holistic design is drastically reduced to only 500. The presented optimization architecture also accelerates the process, producing results in 35 CPU hours. The overall number of function evaluations for complex compressor design can be kept below 1000 simulations. In conclusion, the proposed strategy is very promising for application in future heat pump design with high potential for further research.
[DOI: 10.1115/1.4069927]

1 Introduction

The electrification of industrial process heat is a crucial step to decarbonize industrial sectors and reduce CO_2 emissions. Heat pumps are agreed on to play a key role as they are able to increase energy efficiency and further enable the usage of renewable energy in industry. There are a large number of studies that highlight the importance of this technology. Madeddu et al. [1] underline the potential of electrification in a study that estimates the reduction of emissions to be up to 78%. The applicability of heat pumps is widely studied. Kosmadakis et al. show the techno-economic potential of heat pumps up to 150 °C [2], and Marina et al. give an overview of the European market potential [3]. There is high research potential for high-temperature applications as outlined by Zühlsdorf et al. [4]. They studied Brayton cycles and cascaded cycles and found economic feasibility up to temperatures of 280 °C. The Brayton cycle heat pump has been identified as a solution for high temperature lifts and is progressing toward market maturity [5,6].

The efficiency of heat pumps is a major key to their economic viability, which is achieved through thoughtful integration and optimal design for specific process demands. The heat pump's performance is very much dependent on the efficiency of the components. As an example, in Brayton cycle systems, the best possible combination of turbomachinery and heat exchangers (HEX) needs to be found while design constraints like engine size and costs are met. A sequential design procedure, where the cycle concept for a heat pump is determined first and the components are designed afterwards, leads to suboptimal designs and can be very time-consuming. Major decisions are made during the cycle concept phase, which optimizes cycle parameters based on assumptions about the component performance. Turbomachine and HEX efficiency are unknown at this point and are usually based on experience values. Optimal component designs are derived based on

Turbo Expo: Turbomachinery Technical Conference & Exposition (GT2025), June 16–20, 2025. GT2025.
[1]Corresponding author.
Manuscript received July 3, 2025; final manuscript received July 22, 2025; published online November 27, 2025. Editor: Jerzy T. Sawicki.

design requirements from the cycle concept. Especially in closed cycles, the component performance is strongly interactive. This means that the optimal design of an HEX can have an impact on the compressor and vice versa. Finding the optimal HP configuration through sequential design is iterative and therefore costs a lot of time, while mistakes in the earliest design phases are hard to rectify later. More integrated approaches that consider the continuous feedback between the cycle design and component optimization can overcome this shortcoming. For this reason, holistic design concepts that simultaneously optimize cycle parameters and geometric component designs will have a large impact in developing heat pumps with higher technological and economic potential. These multidisciplinary optimization strategies (MO) aim to integrate detailed component simulations in a single process. The overall system performance is improved as mismatches between turbomachines, HEX, and cycle parameters are avoided. Uncertainties are reduced as less or no assumptions are required, and component efficiencies are based on physical modeling. As an additional advantage, more information about engine size or part load performance is available in the earliest phases of design. The iterative nature of sequential design is reduced, and the design process itself becomes more efficient, and communication between disciplines is improved. As a downside, integrating detailed component analysis increases the complexity of the optimization problem with a high number of variables and large design spaces. These challenges can be coped with by the investigation of optimization concepts for holistic design strategies, which is the focus of this paper.

1.1 Holistic Heat Pump Design Concepts and Related Work. In the field of multidisciplinary system optimization, several general concepts have been proposed. These concepts are primarily explored through test problems, with only a few having been fully implemented in real-world design processes. Specifically, for the application in designing industrial heat pumps, there is a limited amount of research. Most studies are focused on the integration of radial compressor design together with cycle evaluation. The challenge in MO problems lies in managing the local parameters of individual disciplines (components) while coordinating the overall system optimization through interface parameters and constraints to achieve globally consistent designs. Martins et al. compared and classified several architectures for MO problems, distinguishing between monolithic structures, which solve a single optimization problem, and distributed structures, which involve subproblem optimization [7]. As an example for a single level or monolithic structure, the all-at-once (AAO) approach is a straightforward first step to target the problem. AAO only uses a single optimization containing all design variables and controls consistent system designs with matching interfaces via constraints functions. For large problems, this is not a practical approach and distributed structures with multilevel optimization are better suited. In this work, a collaborative design concept (CO) for heat pumps is introduced. CO splits the optimization into a top-level problem and distributed subproblems for each discipline. Braun et al. introduced the CO concept, and several studies have since investigated its further development and performance [8,9]. Sobieski et al. enhanced CO by integrating quadratic response surfaces (RS) to improve performance [10]. Response surfaces (or surrogate models) are computationally less expensive than detailed component analysis, which is crucial since the subproblems must be solved efficiently.

Application studies of MO have been primarily performed in the fields of aero-engine design [11] and organic Rankine cycles [12]. Hendler et al. compared two optimization approaches for the coupled design of a multistage compressor and combustion chamber of an aircraft engine [13]. They applied both all-at-once optimization and a decoupled approach with geometric interface parameters. The holistic approaches resulted in overall improved designs in terms of fuel consumption and efficiency. In the area of heat pump design, only a limited number of studies have addressed the simultaneous optimization of the system and its components. Typically, when complex analyses are considered, the integration of single components is conducted. In most cases, there is only little focus on the optimization concept itself. For example, Meroni et al. optimized cycle performance and heat flowrate for different working fluids by integrating a meanline-based radial compressor design [14]. Giuffre et al. applied a surrogate model for rapid evaluation of an integrated radial compressor design, thereby accelerating the multi-objective optimization process [15]. By using artificial neural networks instead of the simulation, they were able to decouple the compressor design and effectively reduce the number of function evaluations required. Schiffmann integrated the design of a turbocompressor into the optimization of a domestic air-based heat pump, focusing on enhancing seasonal system efficiency and rotordynamic stability [16]. Schaffrath et al. evaluated the computational fluid dynamics (CFD) based design of radial steam compressors within a two-stage reversed Rankine cycle. They improved convergence by employing a multifidelity (co-Kriging) optimization approach [17]. These studies all underline the potential benefits of holistic heat pump design concepts.

1.2 Use Case: Brayton Cycle Heat Pump. A heat pump based on the reversed Brayton cycle is designed for the holistic optimization studies demonstrated in this paper. The cycle layout is shown in Fig. 1. High temperature lifts and sensible heat transfer with steep temperature profiles are typical application areas for this type of heat pump. These characteristics were considered to define the present use case. For instance, Carnot batteries require highly efficient components, making heat pump configurations with axial turbomachines potentially suitable for this particular application. A compact overview of the working principle is as follows: Air is compressed (1 → 2) to raise the temperature at the primary side inlet of the heat sink heat exchanger (HTHX). On its secondary side, air is heated from 100 °C to 320 °C (9 → 10). This flow is a process requirement and thereby a fixed boundary condition in the design studies. Downstream of the heat sink, the fluid is further cooled down by the recuperator transferring heat to the compressor inlet (3 → 4) functioning as internal heat recovery that is applied to prevent high pressure ratios. A turbine is used to expand the fluid (4 → 5) before it is heated up by making use of the heat source energy (5 → 6). The cycle is closed by flowing through the recuperator to the compressor inlet. In order to design this heat pump, cycle parameters like mass flow, pressure levels, and temperatures at each station need to be optimized together with matching component designs. In holistic optimization, cycle design and component optimizations are performed simultaneously. The gray parameters in Fig. 1 are variables that are determined during this process, while all black values are considered as constants. On the primary side of the cycle, only the inlet pressure of the compressor and the turbine efficiency are fixed. With the compressor and three heat exchangers, multiple components are

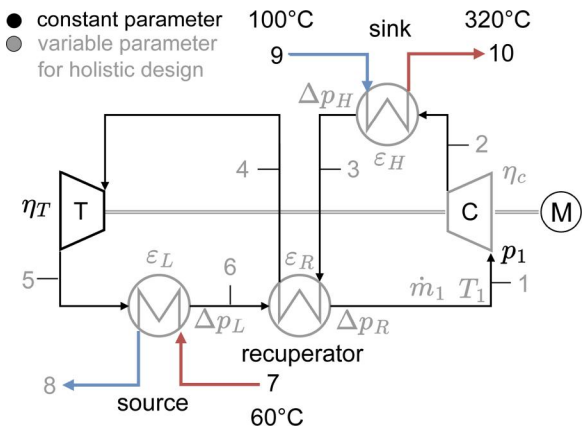

Fig. 1 Use case for holistic heat pump optimization. Reversed Brayton cycle with recuperation.

designed to be optimally matched in the best cycle configuration. The turbine design is not integrated at this point. This is because an adaption of a complex aerodynamic turbine analysis to be functional in holistic design is out of scope for this work and part of future studies.

1.3 Previous Work, Contribution, and Research Questions. The benefits of holistic heat pump design compared to the conventional sequential procedure have been previously demonstrated by the authors of this work [18]. Finding efficient and reliable MO strategies will have a large impact on the design processes of future heat pump systems, enabling their full potential and reducing uncertainties. The formulation of the optimization architecture to distribute analyses to subproblems is a key step. Using an all-at-once approach has not proven to be effective for detailed multicomponent design failing mainly in controlling the constraints responsible to find consistent system configurations. Decoupling the heat exchanger design did significantly improve convergence and reproducibility. As the high dimensional compressor design is still solved on the top level, a high number of approx. 2000 iterations is necessary to reach convergence. This high number should be avoided for two reasons: First, costly function evaluations of component analyses should be minimized. Second, when surrogate supported optimization is used as the top-level optimizer, the training of these models can become very expensive with growing databases and create a bottleneck for the optimization process. Therefore, decoupling the compressor design and reducing the dimensionality of the MO problem is one of the objectives of the present research. A collaborative design structure is introduced for heat pump optimization. As the component optimization subproblems need to be solved repeatedly, their functional output is approximated with computational inexpensive surrogate models. The following research questions are addressed:

- Does a surrogate-based multilevel optimization concept reduce the overall number of expensive function evaluations compared to previously studied holistic architectures?
- Which combination of sampling strategy and regression method is most accurate to predict the functional output of complex component analyses?
- What size of the sampling database is required to prevent high approximation errors?

2 Heat Pump Disciplinary Analyses

The multidisciplinary optimization is based on combining several disciplines at varying levels of fidelity and modeling depth. The cycle performance is assessed on system level. On component level, detailed models are applied to simulate specific disciplines like aerodynamics or heat transfer. Each modeling approach to simulate a single part of the multidisciplinary architecture is referred to as a disciplinary analysis. Each analysis is adapted to be compatible with the MO approach concerning its parameterization and interfaces. An overview of integrated modeling approaches is presented in Secs. 2.1–2.3.

2.1 Cycle Analysis. The analysis of the thermodynamic cycle is performed with TesPy as introduced by Witte and Tuschy [19]. The simulations are based on 0D steady-state modeling setting up an equation system consisting of fixed boundary conditions and variable parameters. It is solved using a Newton–Raphson method calculating all thermodynamic state variables at each station of the cycle. The parameterization of the model is setup by the user and is an essential step to enable its applicability to the specific heat pump design problem. In this work, the process flows on secondary sides of heat sink and heat source HEX remain unchanged as boundary conditions. The heat sink is a process requirement and both in- and outflow of the HTHX are constants. For the heat source, only the inflow conditions are constant. The transferred heat, and thereby the outlet temperature T_8, is determined by the heat pump and the integrated LTHX design. Additionally, the inlet pressure of the compressor and turbine efficiency are constant parameters, as turbine design is not integrated. The model is parameterized so that the efficiency parameters of each component can be specified as boundary conditions, which is a requirement for ensuring its compatibility with the applied optimization architecture. From the perspective of holistic optimization, these values are design parameters. All remaining station values are variables in the cycle model's equation system (e.g., temperatures and pressures) and are determined by the solver. Interfacing parameters to the component analyses are serialized to be used as design points for compressor and heat exchanger design. Cycle analysis is a method with low computational effort and usually converges in seconds.

2.2 Multistage Compressor Analysis. For the aerodynamic compressor design, a sophisticated in-house throughflow environment called ACDC (advanced compressor design code) is adapted for holistic heat pump design. ACDC consists of an S2 streamline curvature flow solver and features a design mode, in which loss correlations and outflow angles are tuned based on models trained with simulations of a pre-optimized airfoil family [20,21]. The throughflow analysis has been widely applied to compressor design studies and is validated with results from CFD as well as experimental data [22]. The process of generating a compressor design starts with the definition of flowpath geometry and compressor topology. A 2D mesh is generated, and the flow field is computed for user-defined inlet conditions and blade design requirements for rotor and stator. For rotors, the target pressure ratio is set, and for stators, the outflow angle. Values for efficiency and numerous flow and stability coefficients are calculated in post-processing routines. For the integration in holistic optimization structures, the design process needs to be flexible for varying inlet conditions that are the results of cycle simulations for individual heat pump configurations. For this reason, ACDC has been extended to be able to cover a large variety of design points and pressure ratios. The design process starts with a generic generation of the geometry, assembling a user-defined number of stages. Hub and shroud lines are generated with deviation splines relative to a reference design. In the next step, the compressor geometry is scaled to match the varying inlet conditions. For the numerical setup of the blade design requirements, spline-based dimensionality reduction is used to interpolate the radial distribution of the target values for each blade. Further information of this procedure can be found in Ref. [23].

A four-stage compressor design as a result of holistic heat pump optimization is visualized in Fig. 2. The design is fully described with a parameter vector $\boldsymbol{p}_C \in \mathbb{R}^{35}$. The execution of each analysis lasts up to 25 s, which means that an optimization of the compressors' design can take up to several hours. Consequently, finding compressor designs with many design parameters is a major challenge in the context of MO approaches, that is addressed as part of the present work.

2.3 Heat Exchanger Analysis. The heat exchanger analysis is performed with in-house tools based on the NTU-method (number of transfer units) to compute heat transfer in shell and tube heat exchangers [24]. Additionally, pressure drop on the tube side and in cross-flow zones of the tube bundle are calculated. The parameter vector to describe each HEX geometry consists of five variables

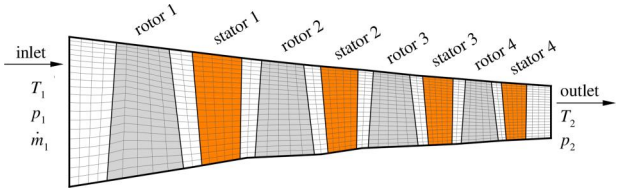

Fig. 2 Multistage axial compressor generated from scratch in holistic heat pump design

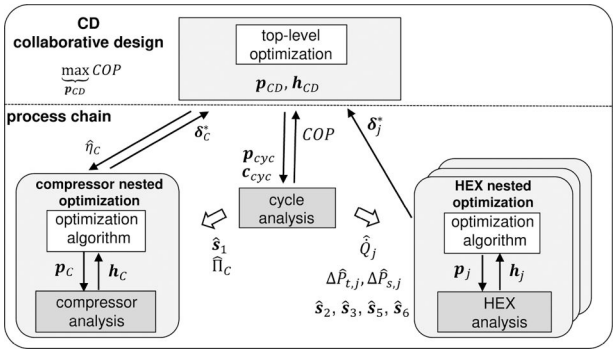

Fig. 3 Architecture of collaborative heat pump optimization

$\boldsymbol{p}_{\text{HEX}} \in \mathbb{R}^5$. Tube length, number of tubes, tube diameter, tube separation, and baffle spacing are set for HEX rating. With the inflow conditions on both sides of the heat exchanger as additional input, the outflow is computed based on the geometric configuration. This analysis is also introduced in more detail in Ref. [18]. The design process to find optimal heat exchanger configurations for HTHX, LTHX, and recuperator takes up to 5 min. It is based on well-established, robust approaches to approximate heat transfer and pressure drop to find feasible designs for specific requirements. For a more detailed analysis, HEX design can be replaced with methods that require higher computational effort for various types of heat exchangers. This is why the minimization of the number of function evaluations to find a matching HEX design in the context of holistic optimization strategies is one focused aspect of this work.

3 Optimization Strategy

In this paper, a holistic heat pump optimization structure with distributed component designs is introduced. A multilevel approach is applied, which means that there is a so-called top-level optimization for the overarching MO problem that orchestrates subproblem optimizations for the component designs. Specifically, the compressor and heat exchanger optimizations are performed in nested subproblem processes. In Secs. 3.1 and 3.2, the optimization architecture and the applied algorithms are presented. The coordination of interfacing parameters for each disciplinary analysis as well as communication mechanisms between top-level and subproblem optimization are described.

3.1 Collaborative Heat Pump Design. A collaborative optimization concept is proposed for the design of reversed Brayton cycle heat pumps. This strategy features a decomposition of the optimization problem as shown in Fig. 3. The core concept is that target values for component performance are optimization parameters on the top level. Subordinate optimization loops are then performed for the subproblems of finding component designs that achieve these exact requirements. Target values and system parameters like the mass flow $\dot{m}$ are varied until the optimized heat pump configuration with matching component designs is obtained. In the case of the present use case, the parameter vector $\boldsymbol{p}_{\text{cyc}} = \boldsymbol{p}_{\text{CD}}$ sets up the cycle analysis together with constant parameters $\boldsymbol{c}_{\text{cyc}}$. It is performed to calculate all thermodynamic states of the system, the target pressure ratio $\hat{\Pi}$ as well as the objective function coefficient of performance (COP). Now, all information for the design points and interfacing parameters of the compressor and HEX are available. In a second step of the process chain, nested optimization loops with local parameter vectors $(\boldsymbol{p}_c, \boldsymbol{p}_j)$ and local constraints $(\boldsymbol{h}_c, \boldsymbol{h}_j)$ are executed that check if these components can meet the requested performance criteria. Each component optimization returns a deviation vector $\boldsymbol{\delta}^*$ to the top level, which traces if the targets are reached for the current configuration. On the top level, these deviations are constraint functions to direct the optimizer to the feasible region. The formulation of the optimization problem is given with:

top-level:

$$\begin{aligned} &\max_{\boldsymbol{p}_{\text{CD}}} \text{COP} = \frac{\dot{Q}_{\text{HTHX}}}{\dot{W}_c - \dot{W}_T} \text{ s.t. } \boldsymbol{h}_{\text{CD}} \le \boldsymbol{\zeta}_{\text{CD}}, \\ &\boldsymbol{p}_{\text{CD}} = \left[\hat{\eta}_C, \hat{\boldsymbol{\varepsilon}}_j, \dot{m}_1, \Delta\hat{P}_{t,j}, \Delta\hat{P}_{s,R}\right] \in \mathbb{R}^9, \; j \in \{\text{H}, \text{L}, \text{R}\} \\ &\boldsymbol{h}_{\text{CD}} = \left[||\boldsymbol{\delta}_c^*||_2, ||\boldsymbol{\delta}_H^*||_2, ||\boldsymbol{\delta}_R^*||_2, ||\boldsymbol{\delta}_L^*||_2\right] \end{aligned} \tag{1}$$

compressor:

$$\begin{aligned} &\min_{\boldsymbol{p}_c \in \mathbb{R}^{35}} |\eta_c - \hat{\eta}_c| \text{ s.t. } \boldsymbol{h}_c \le \boldsymbol{\zeta}_c, \\ &\boldsymbol{h}_c = \left[|\Pi_c - \hat{\Pi}_c|, c_{\text{Koch}}, c_{\text{d,max}}, c_{\text{d,min}}\right] \end{aligned} \tag{2}$$

heat exchangers:

$$\begin{aligned} &\min_{\boldsymbol{p}_j \in \mathbb{R}^5} l_j \text{ s.t. } \boldsymbol{h}_j \le \boldsymbol{\zeta}_j, \; j \in \{\text{H}, \text{L}, \text{R}\} \\ &\boldsymbol{h}_j = \left[|\dot{Q}_j - \hat{\dot{Q}}_j|, |\Delta P_{t,j} - \Delta\hat{P}_{t,j}|, |\Delta P_{s,j} - \Delta\hat{P}_{s,j}|\right] \end{aligned} \tag{3}$$

On the top level, the parameter vector consists of target values for compressor efficiency $\hat{\eta}_c$ and HEX effectiveness $\hat{\boldsymbol{\varepsilon}}_j$. The HEX effectiveness is defined as follows: $\varepsilon = \frac{\dot{Q}_{\text{real}}}{\dot{Q}_{\text{ideal}}}$. Additionally, pressure drop targets $(\Delta\hat{P}_{t,j}, \Delta\hat{P}_{s,R})$ and the heat pumps' mass flow $\dot{m}_1$ are set. The cycle analysis is parameterized to compute all missing station values based on this input. Then, the compressor design is performed to minimize the deviation from target efficiency $|\eta_c - \hat{\eta}_c|$ as the objective function. Furthermore, constraint functions $\boldsymbol{h}_c$ for target pressure ratio $\hat{\Pi}_c$, maximum stability c_{Koch} and a range of diffusion coefficients c_{cd} have to be met. Constraints are implemented as quadratic terms that penalize the objective function value if activated. Listed below are two examples for penalty term formulations $\delta(\boldsymbol{p})$ for equality constraints (targets) and inequality constraints of the compressor:

$$\delta_{c,1}(\boldsymbol{p}) = \begin{cases} (\Pi_c - \hat{\Pi}_c)^2 & \text{if } h_{c,1} = |\Pi_c - \hat{\Pi}_c| > \zeta_{c,1} \\ 0 & \text{otherwise} \end{cases} \tag{4}$$

$$\delta_{c,2}(\boldsymbol{p}) = \begin{cases} (c_{\text{Koch}} - \hat{c}_{\text{Koch}})^2 & \text{if } h_{c,2} = c_{\text{Koch}} > \zeta_{c,2} \\ 0 & \text{otherwise} \end{cases} \tag{5}$$

If the local equality constraint $h_{c,1}$ is not fulfilled for the target pressure ratio $\hat{\Pi}_c$ in Eq. (4), the quadratic penalty term $\delta_{c,1}$ is activated. This is setup to happen if the deviation from the desired target value exceeds a tolerance $\zeta_{c,1}$, which is applied for relaxation. Inequality constraints that restrict the feasible region are treated in a similar way, as formulated in Eq. (5) for the example of the Koch stability criterion. When the constraint function reaches the infeasible region, the objective is penalized with the value of $\delta_{c,2}$. All penalty term values are returned as deviation vectors $\boldsymbol{\delta}^*$ to the top-level, where the vector norm is used to trace feasible designs. The heat exchanger subproblem is treated equivalently: The length of each heat exchanger is minimized to find the most compact design. Penalty terms of equality constraints are activated for target heat flowrate $\delta_{\hat{\dot{Q}}}$, target tube side pressure drop $\delta_{\Delta\hat{P},t}$ and target shell side pressure drop $\delta_{\Delta\hat{P},s}$.

3.2 Software and Algorithms. To solve holistic heat pump design problems, an efficient optimization approach for the top-level optimizer is crucial. For this reason, the DLR in-house suite AutoOpti is used, which is widely used for complex problems like turbomachine design [25]. Metamodel-assisted global optimization based on Kriging models can be applied, as well as genetic operators

like mutation or differential evolution. New candidates are determined by a weighted distribution of the search performed either with different acquisition functions for Bayesian optimization or with the genetic operators. Each optimization run starts by creating an initial database with methods from the design of experiments (DoE), which is continuously updated until convergence is reached. All subproblem optimizations, on the other hand, are performed with differential evolution as implemented in the SciPy library [26]. Differential evolution is a widely used algorithm for black box engineering problems, but may require a large number of function evaluations to detect the global optimum [27].

4 Response Surface Training

Using multilevel architectures with distributed component design reduces the dimensionality of the MO problem, but a very high number of function evaluations for component simulation can occur. These simulations can be computationally expensive. As an example, the compressor design using ACDC will take several hours and cannot be performed in subproblem optimizations that need to be repeatedly executed. Surrogate models offer the advantage of being computationally inexpensive to evaluate, which is why the holistic optimization studies in this work are performed with the approximation of the components via regression. Additionally, convergence issues are mitigated in this way, making the integration of surrogates a promising approach for holistic optimization. The method for regression can be chosen freely as long as the model is able to reliably predict the deviation from predefined target values. One of the main objectives of this study is the investigation of suitable regression methods for surrogate model training. To generate an accurate model, the most suitable combination of spatial distribution of sampling points, size of the database, and regression method needs to be determined. Gaussian process regression (GPR) is compared to different approaches of linear regression and radial basis functions (RBF). GPR is a widely used method to robustly approximate complex nonlinear functions. The functional response is treated as a Gaussian distribution: $f(\boldsymbol{p}) = \mathcal{N}(\mu(\boldsymbol{p}), \sigma^2(\boldsymbol{p}))$. In this way, the model is not only able to predict the output with the mean value $\mu(\boldsymbol{p})$ but additionally quantifies the uncertainty with information about the local variance $\sigma^2(\boldsymbol{p})$ [28]. Because of these advantages, GPR is used here as the baseline method. These models are known to work well with smaller datasets [29], which is an important characteristic to minimize overall component function evaluations. The squared exponential kernel function (or RBF kernel) is used as the default with a vector length scale that is optimized during the fitting process. All regression models are trained using classes provided by the scikit-learn library [30].

4.1 Sampling Strategies. The sampling strategy is a crucial step for surrogate model training. The overall objective is to reach efficient space filling for global models or to restrict the area of high resolution to relevant areas for local models. Identifying the optimal tradeoff between the quantity of sampled data and model accuracy is important to save computational costs. Random sampling strategies are inefficient in terms of space filling [31]. Methods from DoE are used instead to distribute points in the design space. For a full factorial design, the required amount of sampled points is directly dependent on the number of design variables and scales badly with higher dimensions [32]. Latin hypercube sampling (LHS), on the other hand, distributes samples independently from the dimensionality and has proven to be an efficient method as a basis for surrogate model training [33,34]. In this work, single-step LHS is used as well as adaptive sampling strategies, which start with an initial model that is iteratively refined based on active learning strategies [35].

The sampling strategies are introduced by training of GPR surrogates with static and adaptive sampling. To highlight the characteristics of each approach, a 2D test function [36] is used for visualization in Fig. 4. The contour plots show the prediction of each GPR model. As a baseline approach, single-step LHS is applied with 50 points in Fig. 4(*a*). Figure 4(*b*) shows the result of sequential LHS (sLHS). Here, an initial model is built with 10 randomly sampled points. The model is refined in epochs, by sampling 100 points on the current GPR model and choose the 10 locations of highest variance. It is refined in 4 epochs and results in a more evenly spatial distribution compared to the random nature of sampled data in Fig. 4(*a*). Another approach applied here is adaptive global refinement (GR). The initial model is updated by obtaining the point with the highest variance. This point is determined with an optimization, which is repeated for every step to update the model. The result in Fig. 4(*c*) indicates an even spatial distribution, with the downside that the entire borders of the design space are explored first, where highest variances usually occur. As a consequence, this method may require a large number of samples with increasing dimensionality. As an alternative, local models can be trained with adaptive sampling as shown in Fig. 4(*d*). The method applied here is called contour estimation (CE) and works similar to GR, except that now the objective to obtain the next sample is a function that indicates the probability of hitting a certain target contour value [37,38]. Sample positioning is aimed to be restricted to regions near contour lines while only areas of highest inaccuracy are explored. The effect is highlighted in Fig. 4(*d*), where samples are placed near the black contour lines.

Figure 5 shows the distributions of model accuracy for five repetitions of global GPR training. The gray box indicates the spread of evaluated outputs, the black line is the median and the triangle represents the mean value. Also, the error bars are a measure for the confidence interval. The metrics are the coefficient of determination R^2 and the mean absolute error MAE with regard to predictions for a fixed test dataset. It can be deduced that compared to single-step LHS, the adaptive approaches improve the global fit of the model. Overall sLHS shows the best accuracy, which is caused by the tendency of GR to explore the borders so that the sample points are spatially further apart. The high variance of the adaptive sampling strategy in Fig. 5(*b*) can be explained with the fact that the initial LHS is randomly generated each time and has a large impact on the final model.

4.2 Adaptive Sampling With Detection of Infeasible Regions. Some simulation methods for component analysis show convergence issues for infeasible configurations. This means that

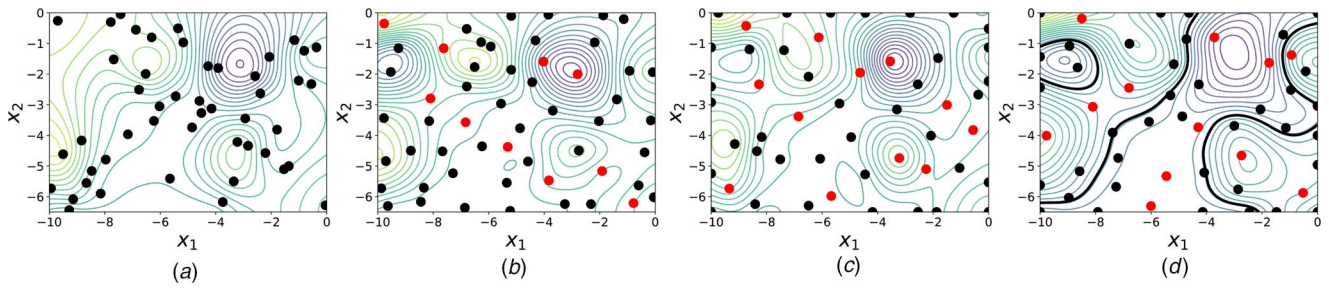

Fig. 4 Sampling strategies for GPR training demonstrated with Mishra's bird function: (*a*) static LHS, (*b*) sequential LHS, (*c*) global adaptive refinement, and (*d*) contour estimation. Overall samples: 50.

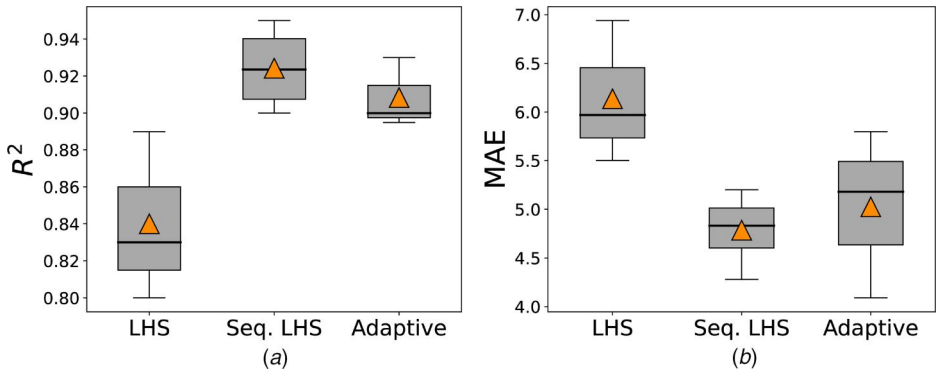

Fig. 5 Box plots of model accuracy metrics for global sampling approaches

they will not provide a return value if the solver fails to converge. This is an additional challenge for adaptive training of surrogate models, as the search for promising sample points needs to avoid regions that are not likely to converge. To overcome this, a concept is introduced, where a second model is trained that predicts if the analysis is likely to converge or not. This is achieved by using a support vector machine classifier (SVC, scikit-learn [30]) to predict feasibility. SVC is characterized by low training effort and is effective for high dimensional problems and small- to medium-sized datasets [39]. The combined approach of classifier and regressor is used for adaptive model training to approximate the complex compressor analysis. In contrast to the HEX analysis used in this work, this simulation method deals with convergence issues.

The procedure is as follows: After creating the initial model, the next sample point is searched in the same way as introduced in the adaptive concepts before (see Sec. 4.1) with the difference, that now a penalty is added to the objective, if the SVC decision function predicts a low probability of convergence. In a next step, the training dataset needs to be updated with the actual function output. If the analysis converges, regression model and SVC model are updated. In case that the analysis does not converge, only the classifier receives an update. This loop is repeated until the training of the model is finished with regard to a user-defined criterion like maximum number of sample points.

Figure 6(*a*) shows the GPR prediction of the compressor efficiency. For testing purposes, only two design parameters are considered: Deviation from reference pressure ratios of the first two rotors of a 4-stage axial compressor is varied to study the functional response. The optimal efficiency is close to the values near $\boldsymbol{p} = [1, 1]$, which is expected as an already optimized reference design is used here. Adaptive global sampling is performed and leads to a very even distribution of samples, which only cover the feasible part of the design space. The decision function of the SVC classifier is shown in Fig. 6(*b*). Nonconverged samples are highlighted as red points. Two things can be derived: First, the decision function separates feasible and unfeasible regions smoothly and reaches values below 0 if convergence is unlikely. Second, the functionality of the adaptive refinement strategy is evident, as samples are placed more densely near the border of feasibility and areas far outside of converged points are not explored. In conclusion, the combination of regression and classification is working for adaptive model training. However, for the high-dimensional compressor analysis, the construction of a globally refined model would require high a number of samples. As an alternative, local models with an assumption about a range of target pressure ratios can be trained. This deals also as a preparation for future work, where surrogate models will be refined during runtime of the top-level optimization and avoiding configurations that are unlikely to converge is an important aspect to efficiently update the subproblem surrogate models.

4.3 Heat Exchangers Response Surfaces. For all three heat exchangers in the system, models are trained to predict the heat flowrate $\dot{Q}$ and the pressure drops on tube side ΔP_t as well as shell side ΔP_s. The training parameters consist of the five geometric design parameters and the inflow conditions, as they are variable during holistic heat pump design. For the HEX of heat sink and heat source, this adds up to eight parameters $\boldsymbol{p}_{\text{train,j}} = [\boldsymbol{p}_j, \dot{m}_{\text{in,t}}, P_{\text{in,t}}, T_{\text{in,t}}] \in \mathbb{R}^8$, as only the inflow conditions on the tube side are variable. The recuperator model needs to be trained with 10 parameters $\boldsymbol{p}_{\text{train,R}} = [\boldsymbol{p}_R, \dot{m}_{\text{in,t}}, P_{\text{in,t}}, T_{\text{in,t}}, P_{\text{in,s}}, T_{\text{in,s}}] \in \mathbb{R}^{10}$, as it is fully connected to the heat pump cycle and inflow conditions on both sides are variable. In order to investigate methods of regression, different sizes of sampled data are generated with the HEX analysis using LHS. GPR with different kernel functions and sampling

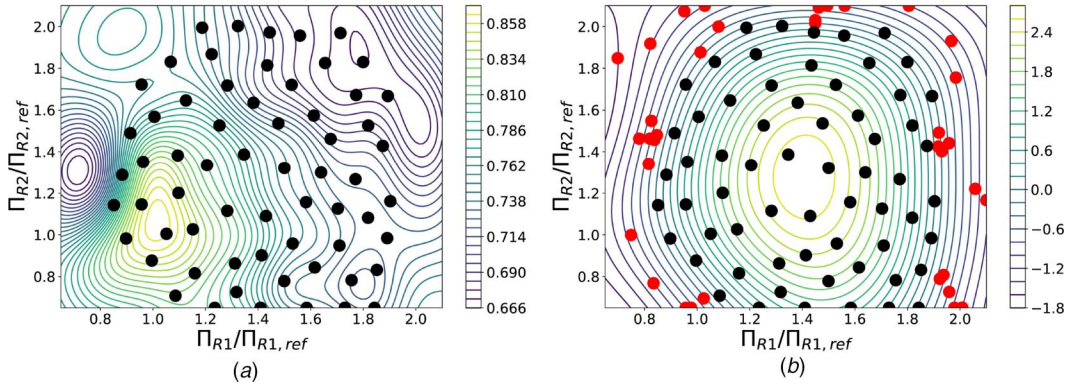

Fig. 6 Example of global adaptive sampling with restriction of nonconverged regions. (*a*) GPR prediction of compressor efficiency. (*b*) Decision function of the classifier.

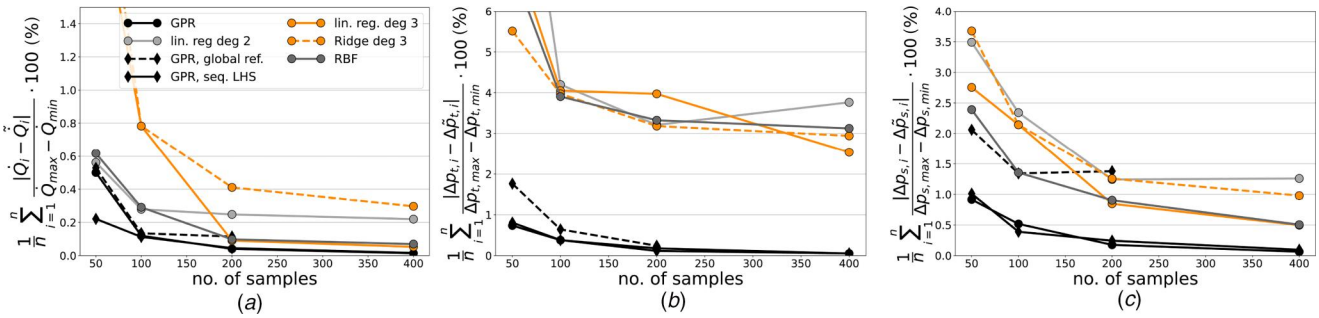

Fig. 7 Comparison of relative mean absolute error of heat sink HEX models depending on method of regression and sampling strategy. (*a*) $\dot{Q}_H$, (*b*) $\Delta P_{t,H}$, (*c*) $\Delta P_{s,H}$. Test data consists of 5000 samples.

strategies is compared to linear regression and RBF using the same database in case of single-step model generation.

Figure 7 shows the comparison of the model accuracy with the metric absolute mean error normalized to the output range of the model. For all output functions, a similar trend can be derived: The black lines representing the accuracy of the GPR models indicate the best fit over the entire range of investigated sampling quantities. Very high accuracy is reached if more than 200 samples are used for model training. Two additional things can be concluded for the GPR models: The dashed line indicates that adaptive global refinement as a sampling strategy is not beneficial in this case. This can be explained by the fact mentioned before, that global refinement tends to explore the borders of the design space first, so that a high number of samples would be needed for high accuracy. Because of the high training effort of GR, the sample size is limited to 200 for this strategy. As a second point, sLHS sampling does primarily show significant advantages for sampling sizes with less than 100 points. For the linear models, three regression approaches are compared. Polynomials of degree 2 and 3 are trained with all interaction terms. In addition, Ridge regression is applied, which uses regularization by adding a penalty term to the objective, which is used to fit model coefficients aiming to prevent overfitting for smaller datasets [40]. The linear model of degree 3 delivers the overall best fit when more than 200 sampling points are used. The model consists of 165 coefficients, which explains worse fit with little sampling data, also compared to the linear model with degree 2. Ridge regression is not beneficial here and delivers a worse fit. The best linear model reaches similar accuracy compared to GPR for the prediction of $\dot{Q}$ but performs worse for the pressure drops. RBF interpolation is analyzed as the last method. It is a kernel-based method that computes the similarity between points based on their distance in the input data [28]. A Gaussian kernel is used for these studies. The model performs very similarly to the best linear regression and reaches overall comparable accuracy. The results underline the capability of GPR to robustly reach good fits with small sampling datasets. More training data would be needed to improve the prediction of pressure drops for linear regression.

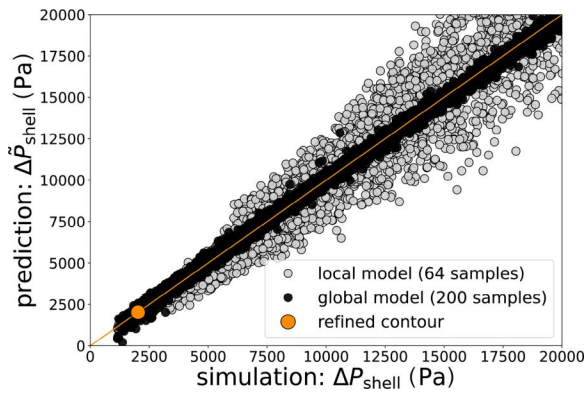

Fig. 8 Comparison of local and global models for prediction of shell side pressure drop

For some applications, the training effort can potentially be reduced by using local models, which only reach high accuracy in relevant areas. As an example, the heat flowrate of the sink HEX or pressure drop on secondary sides can be considered as constants, as they are defined by the process demand. In this case, the model is not required to predict the entire range of possible function values but can be limited to specified contour values. Figure 8 shows the parity between predicted and simulated values of the shell side pressure drop comparing a local to a global model. The local model has been trained with the previously introduced adaptive contour estimation method for a target pressure drop. It reaches similar local accuracy with only 64 samples used for training, while the global model is generated with 200 samples. Due to the local character, the accuracy decreases with increasing distance to the contour value.

4.4 Compressor Response Surfaces. The response surfaces of the compressor are trained with parameter vectors of 37 dimensions $\boldsymbol{p}_C \in \mathbb{R}^{37}$. These consist of 35 geometric design parameters, and additionally, the values of inlet mass flow and temperature are considered, which are varied during holistic heat pump design. The inlet pressure is not considered a design parameter in this work. The number of training samples is limited to 2000. The choice of this quantity is related to the objective of this research, to minimize the number of function evaluations for detailed component analyses in order to avoid high computational effort, also with regard to future applications. The approach to investigate the regression methods is similar to that introduced in the HEX section before. Four datasets with 250, 500, 1000, and 2000 samples are generated with LHS and used for training of all static models. Global adaptive refinement is not considered here, as the training effort would be too high. Adaptive sampling with the sLHS method is performed by epochal selection of samples from the largest dataset that are most likely to improve model quality.

The comparison of model accuracy is again analyzed with the relative mean absolute error in Fig. 9, comparing GPR, linear regression, and RBF. For the prediction of pressure ratio and isentropic compressor efficiency, GPR delivers the best fit for all sizes of sampling data. Using the Matern kernel brings an additional improvement for accuracy. The same accounts for applying sLHS, which is here the superior sampling strategy showing a larger effect on improving the prediction of the efficiency. In contrast to the HEX models, the linear models profit significantly from regularization for this dimensionality. Applying Ridge and Lasso regression improves the model quality drastically. This is because of the high number of model coefficients, and overfitting to training data needs to be avoided. Degree 2 models perform better than third degree, which can also be explained by the increasing number of coefficients for higher order models, which perform worse with smaller sets of training data. RBF models provide a similar fit compared to Ridge regression. Lasso regression leads to an improvement, especially close to 1000 sample points. In general, the pressure ratio is predicted with a smaller uncertainty compared to the efficiency,

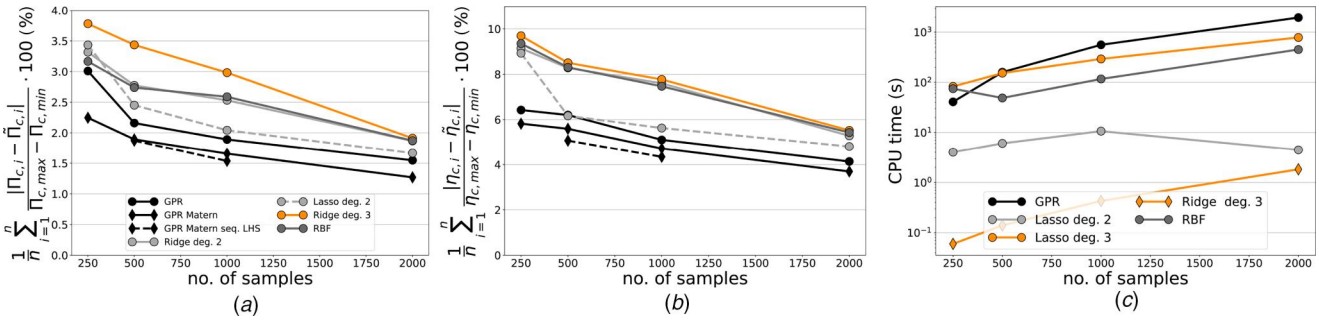

Fig. 9 Comparison of relative mean absolute error of compressor models depending on method of regression and sampling strategy. (*a*) Π_c, (*b*) η_c, (*c*) training effort. Test data consists of 500 samples.

which can be explained by the lower number of design variables that show high sensitivity for this model output. The computational effort is shown in Fig. 9(*c*). GPR requires the highest CPU time, which is caused by inversion of the covariance matrix, where the effort grows cubically with the number of samples. Linear models with Ridge regression are very fast, even for the third-order model. Lasso and RBF also show higher training effort, which is partly caused by the use of cross-validation schemes for parameter tuning. In summary, the studies underline that GPR is the most reliable method to provide accurate predictions for the component analyses used in this work.

5 Holistic Optimization Study

A Brayton cycle heat pump is designed with the introduced collaborative design strategy. To avoid excessive computational costs, this multilevel approach is performed using surrogate models to replace the component analyses. The functional output of the heat exchangers is approximated using GPR models with sLHS sampling and a database of 400 points. For the compressor, GPR models with 1000 samples are applied, as they provide a good tradeoff between model accuracy and training effort. The Matern kernel function and sLHS sampling are used to train overall 5 models. Collaborative heat pump optimization is then performed using a Kriging assisted optimizer (AutoOpti) on top-level. Five optimization runs are executed to test convergence and reproducibility of results. In a last step, the approximation error of the models is investigated by evaluation of the optimized component parameter vector with the actual component analysis to determine the local accuracy of the predictions.

5.1 Convergence and Reproducibility. One of the main challenges of performing holistic heat pump design is the high number of parameters of each disciplinary analysis that make the MO problem increasingly challenging with growing numbers of integrated components. In previous work, the high-dimensional compressor design was handled by the top-level optimizer, and HEX were matched in nested optimization loops [18]. As a consequence, the top-level optimizer needs, in average, more than 2000 iterations to converge. There are two reasons for this: First, the compressor design is a complex problem with many parameters, while at the same time, constraints for consistent cycle configurations with matching HEX designs need to be controlled. Second, convergence issues caused by the direct integration of analyses can be problematic.

Collaborative design as a distributed optimization architecture leads to significant improvements. Figure 10 shows the convergence of the objective function COP, which is achieved within less than 500 top-level iterations. This is the consequence of reducing the complexity of the top-level problem, which now mainly deals with obtaining the best target values for component efficiencies. The gray area on the left side marks the initial randomly generated DoE with LHS. After these first 60 evaluations, the optimization starts and invokes a steep improvement of the objective. The orange symbols are the predictions of the Kriging metamodels used for the top-level

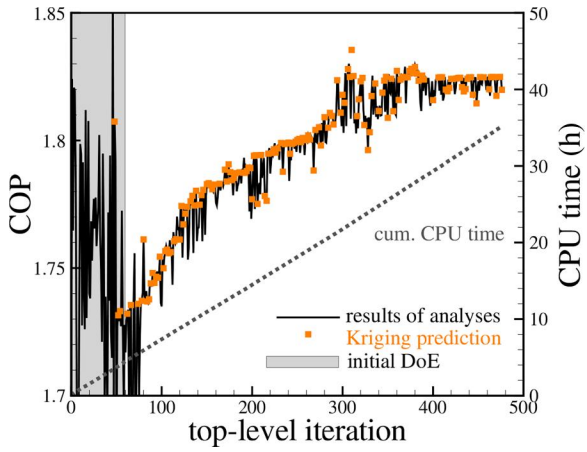

Fig. 10 Convergence of Kriging assisted holistic heat pump optimization

optimization, which turn out to be spot on. In combination, these observations indicate that the orchestration of optimization algorithms together with the proposed optimization architecture is well-suited for holistic design. Furthermore, the cumulative CPU time including surrogate model training is approx. 35 h, which is very fast in context of multidisciplinary heat pump design integrating multiple components.

Figure 11 compares the relative deviations from the mean values of selected parameters for each optimization run. Overall, a very good reproducibility can be concluded. The relative deviations for the range of objectives (COP*) are within an interval of approx. 1%. Even smaller are the deviations of compressor efficiency, which underlines that the subproblem optimization approach is advantageous. A larger spread occurs for the mass flow cycle parameter but

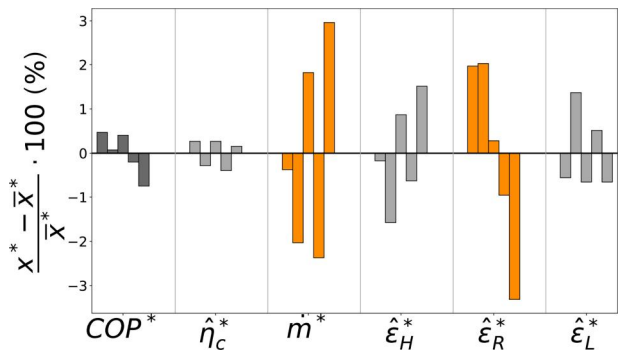

Fig. 11 Comparison of relative deviation from mean values for COP and selected optimization parameters. Each bar represents one of five runs of collaborative heat pump design.

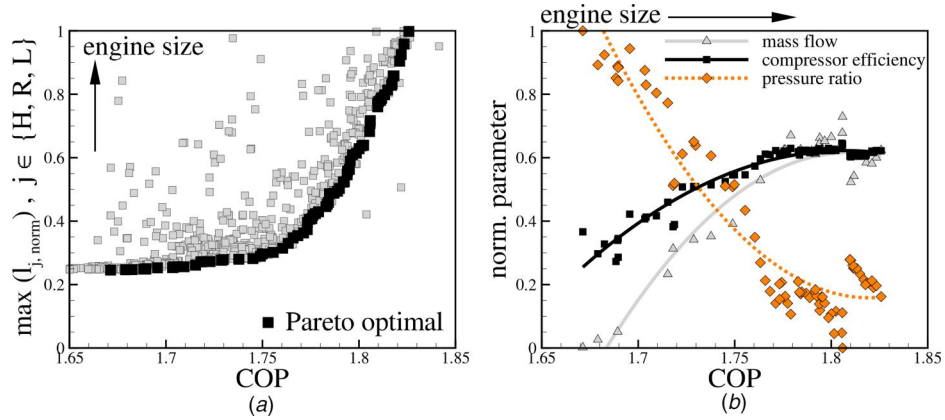

Fig. 12 Multi-objective optimization for COP and minimum length of HEX. Normalized parameters: $x_{norm} = \frac{x - x_{min}}{x_{max} - x_{min}}$. (*a*) Pareto optimal results showing tradeoff between efficiency and engine size. (*b*) Parameter trends for Pareto optimal heat pumps.

it is still in a narrow range of approx. 5% variation. The same accounts for HEX effectiveness, which is in the case of sink and source HEX directly dependent on the mass flow ratio to the process side. Thus, these deviations are directly interacting with variations of the mass flow. The largest spread can be identified for the recuperator, which is also the HEX that is the most complex to design.

To underline the potential of holistic design concepts, Fig. 12(*a*) shows a multi-objective optimization study additionally considering the engine size together with the COP. The Pareto optimal configurations highlighted in black clearly indicate the tradeoff between compactness of the engine and its performance. More compact engines, meaning those with small values for maximum HEX length, show worse performance with lower COP values. Heat pump designs with a larger engine size, on the other hand, show increased performance. Holistic optimization approaches providing this detailed geometric information in early stages of design can thereby drastically improve decision-making, as the available installation space can be a crucial design constraint in an industrial environment. The functionality of the introduced holistic concept is supported by the analysis of trends for selected cycle parameters in Fig. 12(*b*). For Pareto optimal heat pumps, more compact designs are showing lower mass flows and higher pressure ratios. These are necessary to compensate for deteriorated HEX effectiveness with higher outlet temperatures of the compressor. The interactive dependency of compressor design on these cycle parameters is also evident, as a decline in efficiency with increasing pressure ratios is shown.

5.2 Evaluation of Model-Specific Local Approximation Errors. An open question remains regarding the local accuracy of the component surrogate models. Possible exploitation of model inaccuracies by the subproblem optimizers has to be avoided. The following procedure is applied to assess the reliability of the models near the identified optimal heat pump configuration:

(1) Design target values for the compressor and HEX are adopted from the top-level optimizer for the best heat pump configuration. For HEX, these include inflow conditions and targets for heat flow $\dot{Q}$ and pressure drops $\Delta\hat{P}_i$. Equivalently, for the compressor, these design points consist of inflow values and targets for efficiency $\hat{\eta}_c$, pressure ratio $\hat{\Pi}_c$, and stability coefficients.
(2) The optimized parameter vectors $\boldsymbol{p}^*$ are determined by designing the components according to the predictions by the surrogate models for the design points defined in step 1.
(3) Each parameter vector $\boldsymbol{p}^*$ is evaluated with the actual component analysis and the approximation error is calculated:

$$e_a = |(1 - (x/\tilde{x})| \cdot 100\,[\%]$$

The local approximation errors for heat sink HEX models in the holistically optimal design point are listed in Table 1. The subproblem optimizations are repeated 6 times, and the approximation error e_a is determined for each run. This procedure is applied due to the fact that multiple designs can possibly meet the demands of the target values and consequently lead to different errors. The mean value of the error and its standard deviation σ are listed for all approximated HEX functions. GPR models with sLHS sampling have been used for the holistic optimization study and reach the best overall local accuracy, as indicated in the second line. Heat flowrate and pressure drop predictions are spot on. In addition, the standard deviations are very low, which means that for each run, almost identical values are obtained. This is overall a very good result. For reasons of comparison, errors for alternative models are evaluated here as well: The GPR model with LHS sampling works well except for ΔP_t, where minor deviations occur. The locally trained GPR shows the trend of slightly increased errors but delivers overall accurate predictions for these design conditions. Hence, local models for heat exchangers are an alternative to reduce training effort with fewer function evaluations. As already indicated by the analysis of global model accuracy, the linear regression model performs worse in all cases. A linear model with a degree of 3 is evaluated and the prediction of the pressure drop is imprecise for both sides. RBF performs significantly better, reaching the lowest overall error for the heat flowrate $\bar{e}_{\dot{Q}}$ but reveals deviations for the pressure drop predictions. In conclusion, the results indicate that the GPR models are well-suited for the prediction of HEX outputs with

Table 1 Local accuracy of HEX response surfaces in optimal heat pump design points: Mean value and standard deviation of approximation errors *e* (%)

Model	$\bar{e}_{\dot{Q}}$	$\sigma_{e,\dot{Q}}$	$\bar{e}_{\Delta p_t}$	$\sigma_{e,\Delta p_t}$	$\bar{e}_{\Delta p_s}$	$\sigma_{e,\Delta p_s}$
GPR LHS	0.08	3.2×10^{-5}	4.88	0.01	0.86	7.8×10^{-3}
GPR sLHS	0.06	5.5×10^{-5}	0.82	0.7×10^{-3}	1.22	2.8×10^{-3}
GPR local	0.05	0.05	5.81	1.06	6.68	9.62
RBF	0.03	5×10^{-4}	11.8	1.1	8.9	1.88
lin. regr.	0.12	0.01	19.89	1.93	24.98	27.31

400 sampling points for all global models.

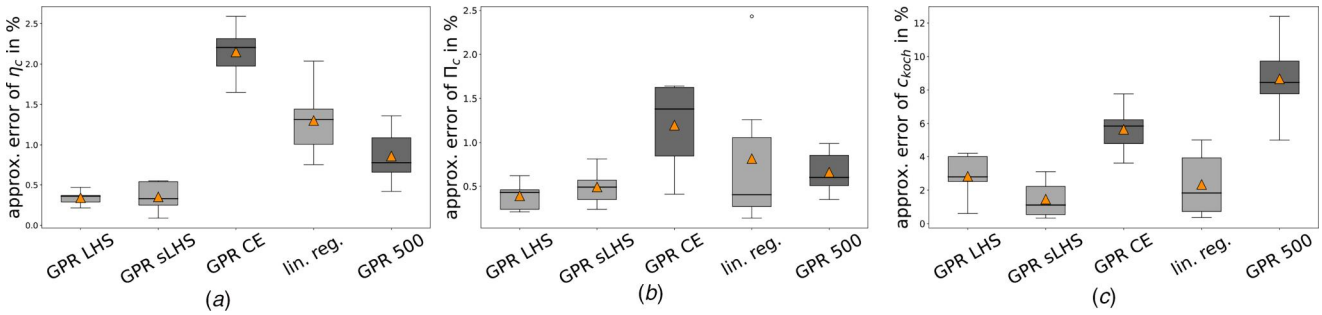

Fig. 13 Local approximation errors of evaluated designs for: (*a*) compressor efficiency, (*b*) pressure ratio, and (*c*) stability criterion. 1000 sampling points for all global models.

an acceptable risk of inaccuracy. The CPU time to perform these subproblem optimizations with GPR is in average 12 s. The physics-based analysis takes 3–5 min., so even for the relatively fast HEX evaluations surrogates can speed up the subproblem process significantly. In perspective, the heat exchanger analysis will be replaced with more detailed modeling, which means the effect will become more significant.

This is already the case for the compressor optimizations. Using GPR response surfaces, convergence is achieved within less than 2 min to find matching designs for the specified target values. Using linear regression is even faster, with an average duration of 50 s. If the same optimization with the identical number of function evaluations had been performed directly with the aerodynamic analysis, this process would take approx. 180 h. As this process needs to be repeated for each top-level iteration, the importance of using response surfaces for multilevel optimization structures becomes evident. The approximation errors for this discipline are visualized in Fig. 13. The trends of the local model quality are similar to the analysis of the HEX models before. Overall, the GPR models reach good agreement with the physics-based analysis. Global GPR using LHS and sLHS are trained with 1000 samples and show similar errors for both efficiency η_c and pressure ratio Π_c. For testing purposes, the local GPR model (GPR CE) has been trained with 500 samples near a fixed pressure ratio contour. The correct contour value is unknown at the time of training as the optimal pressure ratio is a result of the holistic system design. Consequently, this model shows higher inaccuracies and a larger spread of the results. The same trend accounts for the linear model, which shows significantly higher errors compared to the GPR models (GPR LHS, GPR sLHS) using the identical database. Also, an outlier occurs for the prediction of the pressure ratio in Fig. 13(*b*). For comparison, a GPR model with 500 samples is shown. As expected, the smaller sampling size decreases the accuracy for all predictions. While efficiency and pressure ratio are generally predicted quite accurately, the stability criterion c_{Koch} shows larger errors for all models. Here, sLHS sampling seems to bring slight advantages. Comparing the models, the trends still remain similar, as smaller databases and using linear regression instead of GPR invokes worse accuracy and wider confidence intervals.

In conclusion, it can be stated that response surface-based collaborative design is a promising approach to conduct holistic heat pump optimizations. However, potential model inaccuracy is critical, as the optimizers may exploit local model deviations that can lead to imprecise predictions of the component performance or even worse, infeasible heat pump configurations. For these reasons, the multilevel strategies will be further investigated with adaptive models that are locally refined during the runtime of the optimizations to eliminate the risk of significant approximation errors.

6 Conclusions and Outlook

This paper introduces a holistic collaborative design strategy for heat pumps with distributed component optimizations. Its main concept is to define target values for components at top level and solve subproblem optimizations on the component level. Deviation values are returned to the top-level optimizer, which indicate to what extent the target values can be reached. This strategy lowers the dimension on top level of the holistic design problem but also invokes a high number of necessary function evaluations for the distributed problems of component design. The high computational effort resulting from direct integration of detailed component analyses is compensated for by using computationally inexpensive surrogate models. These models predict the functional output of heat exchanger and compressor simulations. Regression methods in combination with single-step and adaptive sampling strategies are compared regarding global accuracy, functionality in holistic design, and local approximation errors. It is found that Gaussian process regression delivers the best fit for the analyses used in this work and is superior compared to linear regression and radial basis functions. This method reaches highest global accuracy for all investigated sampling sizes. The predictions of HEX models with $\boldsymbol{p}_j \in \mathbb{R}^{[8,10]}$ are almost spot on using a database of 400 points with sequential Latin hypercube sampling. The complex models for the approximation of the compressor analysis are trained with a dataset of 1000 samples with $\boldsymbol{p}_C \in \mathbb{R}^{37}$. In this way, sufficient accuracy is reached in a tradeoff with moderate training effort. A holistic optimization study is performed with the integration of these surrogates. Using the collaborative optimization approach enables convergence in less than 500 top-level evaluations. For each iteration, the subproblem optimizations are executed with the response surfaces. These converge in 15 s for the HEX and in less than 120 s to find compressor designs. If the latter were performed directly with the aerodynamic analysis approx. 180 h would be needed for each subproblem. This underlines the importance of using surrogate models, which enable holistic optimization to be realized in 35 CPU hours. The reproducibility of results is very high and similar objectives and heat pump configurations are found in repeated design runs. Relative deviations of the objective function and compressor efficiency are lower than 1%. Local approximation errors are evaluated and are found to be extremely small for the best HEX models. The more complex compressor models indicate higher approximation errors, but sufficient accuracy is reached with consideration of the moderate database. Databases are intentionally kept to the upper limit of 1000 training samples, as component analyses for holistic design can potentially become computationally more costly. Minimization of function evaluations will enable the integration of high dimensional analysis like CFD. It can be concluded, that multilevel holistic heat pump design is a very promising strategy with high potential for future research. To lower the risk of approximation errors of integrated response surfaces, adaptive surrogate models will be investigated. These models will be refined during runtime of the optimization. An adaptive strategy can potentially further decrease function evaluations and improve the design process by lowering the risk of exploitation of local model inaccuracy. This work already offers valuable insights into the practical benefits of holistic design concepts, supported by a multi-objective optimization study considering engine size and its tradeoff

with the performance. This allows improved decision making if the installation space is limited, which is crucial for identifying the optimal heat pump design. This additionally implies the long-term impact of this work. In future studies, more sophisticated functions for engine size or costs will be integrated based on geometric parameters of varying types of heat exchangers or turbomachines. Beyond that, the integration of turbine analysis or the design of more complex cycles is possible as subproblem optimizations are distributed and can be performed in parallel. Each additional component will add its target design parameters on top-level, which does not create any issues for the applied Kriging assisted optimization. This approach will remain efficient even for significantly higher dimensionality.

Data Availability Statement

The datasets generated and supporting the findings of this article are obtainable from the corresponding author upon reasonable request.

Nomenclature

ACDC = advanced compressor design code
$\boldsymbol{c}$ = constant parameter vector
CO = collaborative optimization
COP = coefficient of performance
DoE = design of experiments
e = approximation error (%)
GPR = Gaussian process regression
GR = global refinement
HEX = heat exchanger
$\boldsymbol{h}$ = constraint vector
l = length (m)
LHS = Latin hypercube sampling
$\dot{m}$ = mass flow (kg/s)
MAE = mean absolute error
MO = multi-disciplinary optimization
P = total pressure (Pa)
PC = process chain
$\boldsymbol{p}$ = design vector
$\dot{Q}$ = heat flow rate (W)
RBF = radial basis function
$\boldsymbol{s}$ = station value vector
sLHS = sequential Latin hypercube sampling
SLC = streamline curvature
S2 = meridional plane
T = temperature (K)
$\dot{W}$ = power (W)

Greek Symbols

$\boldsymbol{\delta}$ = deviation vector
ε = effectiveness
$\boldsymbol{\zeta}$ = relaxation vector
η = isentropic efficiency
Π = pressure ratio
σ = standard deviation

Superscripts and Subscripts

c = compressor
cyc = cycle
H = high temperature heat exchanger (HTHX)
h = hub
L = low temperature heat exchanger (LTHX)
R = recuperator
s = shell
T = turbine
T = tube
$*$ = optimized value
$\hat{}$ = target value
$\sim$ = predicted value

Appendix. Input and Output Parameters

Table 2 Overview of input and output parameters of disciplinary analyses

Compressor analysis

Inputs		Outputs	
Rotational speed	ω	Isentr. efficiency	η
Rotor blade design	$\Pi_R \in \mathbb{R}^{12}$	Pressure ratio	Π_C
Stator blade design	$\boldsymbol{\beta}_R \in \mathbb{R}^{12}$	Koch criterion	$\boldsymbol{c}_{\text{Koch}}$
Taper angles rotors	$\boldsymbol{\alpha}_R \in \mathbb{R}^4$	Diffusion coefficient	$\boldsymbol{c}_{\text{diff}}$
Taper angles stators	$\boldsymbol{\alpha}_S \in \mathbb{R}^4$	Flow coefficient	$\boldsymbol{c}_{\text{flow}}$
Inlet radii	$\boldsymbol{R}_i \in \mathbb{R}^2$		
Inlet conditions	$[\dot{m}, T_1, p_1]$		

Heat exchanger analyses $\text{HEX}_j, j \in H, R, L$

Inputs		Outputs	
Tube length	$\boldsymbol{l} \in \mathbb{R}^3$	Heat flow rate	$\dot{Q}_j$
No. of tubes	$\boldsymbol{n}_t \in \mathbb{R}^3$	Pressure drop tubes	$\Delta P_{t,j}$
Tube spacing	$\boldsymbol{s} \in \mathbb{R}^3$	Pressure drop shell	$\Delta P_{s,j}$
Tube diameter	$\boldsymbol{d} \in \mathbb{R}^3$		
No. of baffles	$\boldsymbol{n}_b \in \mathbb{R}^3$		
Tube inflow	$[\dot{m}_{\text{t},j}, T_{\text{t},j}, P_{\text{t},j}]$		
Shell inflow	$[\dot{m}_{\text{s},j}, T_{\text{s},j}, P_{\text{s},j}]$		

Cycle analysis

Inputs		Outputs	
Mass flow	$\dot{m}$	Pressure ratio	Π_C
Effect. HEX_j	$\boldsymbol{\varepsilon} \in \mathbb{R}^3$	Coeff. performance	COP
Pressure drop tubes	$\Delta \boldsymbol{P}_t \in \mathbb{R}^3$	Station values	T_i, P_i
Pressure drop shell	$\Delta P_{s,R}$		
Heat sink inflow	$[\dot{m}_9, T_9, p_9]$		
Heat sink outflow	$[\dot{m}_{10}, T_{10}, p_{10}]$		
Heat source inflow	$[\dot{m}_7, T_7, p_7]$		

Overall design parameters: $\boldsymbol{p} \in \mathbb{R}^{58}$

References

[1] Madeddu, S., Ueckerdt, F., Pehl, M., Peterseim, J., Lord, M., Kumar, K. A., Krüger, C., and Luderer, G., 2020, "The CO_2 Reduction Potential for the European Industry Via Direct Electrification of Heat Supply (Power-to-Heat)," Environ. Res. Lett., **15**(12), p. 124004.
[2] Kosmadakis, G., Arpagaus, C., Neofytou, P., and Bertsch, S., 2020, "Techno-Economic Analysis of High-Temperature Heat Pumps With Low-Global Warming Potential Refrigerants for Upgrading Waste Heat Up to 150 °C," Energy Convers. Manage., **226**, p. 113488.
[3] Marina, A., Spoelstra, S., Zondag, H. A., and Wemmers, A. K., 2021, "An Estimation of the European Industrial Heat Pump Market Potential," Renewable Sustainable Energy Rev., **139**, p. 110545.
[4] Zühlsdorf, B., Bühler, F., Bantle, M., and Elmegaard, B., 2019, "Analysis of Technologies and Potentials for Heat Pump-Based Process Heat Supply Above 150 °C," Energy Convers. Manage.: X, **2**, p. 100011.
[5] Benvenuti, M., Frate, G. F., and Ferrari, L., 2024, "Evaluating Brayton Heat Pump Potential for Industrial Decarbonisation," J. Phys.: Conf. Ser., **2893**(1), p. 012117.
[6] Oehler, J., Gollasch, J., Tran, A. P., and Nicke, E., 2021, "Part Load Capability of a High Temperature Heat Pump With Reversed Brayton Cycle," 13th IEA Heat Pump Conference, Jeju, Korea, Apr. 26–29, pp. 1–12.
[7] Martins, J. R. R. A., and Lambe, A. B., 2013, "Multidisciplinary Design Optimization: A Survey of Architectures," AIAA J., **51**(9), pp. 2049–2075.
[8] Braun, R., Gage, P., Kroo, I., and Sobieski, I., 1996, "Implementation and Performance Issues in Collaborative Optimization," AIAA Paper No. 96-4017.
[9] Rabeau, S., Dépincé, P., and Bennis, F., 2007, "Collaborative Optimization of Complex Systems: A Multidisciplinary Approach," Int. J. Interact. Des. Manuf. (IJIDeM), **1**(4), pp. 209–218.
[10] Sobieski, I. P., and Kroo, I. M., 2000, "Collaborative Optimization Using Response Surface Estimation," AIAA J., **38**(10), pp. 1931–1938.
[11] Tacconi, J., Visser, W. P. J., and Verstraete, D., 2019, "Multi-Objective Optimisation of Semi-Closed Cycle Engines for High-Altitude UAV Propulsion," Aeronaut. J., **123**(1270), pp. 1938–1958.

[12] Lampe, M., de Servi, C., Schilling, J., Bardow, A., and Colonna, P., 2019, "Toward the Integrated Design of Organic Rankine Cycle Power Plants: A Method for the Simultaneous Optimization of Working Fluid, Thermodynamic Cycle, and Turbine," ASME J. Eng. Gas Turbines Power, **141**(11), p. 111009.
[13] Hendler, M., Lockan, M., Bestle, D., and Flassig, P., 2018, "Component-Specific Preliminary Engine Design Taking Into Account Holistic Design Aspects," Int. J. Turbomach., Propul. Power, **3**(2), p. 12.
[14] Meroni, A., Zühlsdorf, B., Elmegaard, B., and Haglind, F., 2018, "Design of Centrifugal Compressors for Heat Pump Systems," Appl. Energy, **232**, pp. 139–156.
[15] Giuffre', A., Ascione, F., de Servi, C., and Pini, M., 2023, "Data-Driven Modeling of High-Speed Centrifugal Compressors for Aircraft Environmental Control Systems," Int. J. Refrig., **151**, pp. 354–369.
[16] Schiffmann, J., 2015, "Integrated Design and Multi-Objective Optimization of a Single Stage Heat-Pump Turbocompressor," ASME J. Turbomach., **137**(7), p. 071002.
[17] Schaffrath, R., Stathopoulos, P., Schmitz, A., and Nicke, E., 2025, "Multistage Turbomachinery Optimization for High Temperature Heat Pumps With the Reverse Rankine Cycle," ASME J. Turbomach., **147**(11), p. 111003.
[18] Gollasch, J., Lockan, M., Stathopoulos, P., and Nicke, E., 2024, "Multidisciplinary Optimization of Thermodynamic Cycles for Large-Scale Heat Pumps With Simultaneous Component Design," ASME J. Eng. Gas Turbines Power, **146**(2), p. 021015.
[19] Witte, F., and Tuschy, I., 2020, "TESPy: Thermal Engineering Systems in Python," J. Open Source Software, **5**(49), p. 2178.
[20] Schnoes, M., and Nicke, E., 2015, "Automated Calibration of Compressor Loss and Deviation Correlations," ASME Paper No. GT2015-42644.
[21] Schnoes, M., Voß, C., and Nicke, E., 2018, "Design Optimization of a Multi-Stage Axial Compressor Using Throughflow and a Database of Optimal Airfoils," J. Global Power Propul. Soc., **2**, p. W5N91I.
[22] Schnoes, M., Schmitz, A., and Goinis, G., 2019, "Strategies for Multi-Fidelity Optimization of Multi-Stage Compressors With Throughflow and 3D CFD," ISABE 2019, Canberra, Australia.
[23] Gollasch, J., Lockan, M., Stathopoulos, P., and Nicke, E., eds., 2023, "Multi-Disciplinary Optimization of Thermodynamic Cycles for Large-Scale Heat Pumps With Simultaneous Component Design," Proceedings of the Turbomachinery Technical Conference and Exposition, Boston, MA, June 26–30.
[24] Springer-Verlag GmbH, 2013, *VDI-Wärmeatlas*. Springer, Berlin, Heidelberg.
[25] Voß, C., Aulich, M., and Raitor, T., 2014, "Metamodel Assisted Aeromechanical Optimization of a Transonic Centrifugal Compressor," ISROMAC, Honolulu, Feb. 24–8, p. 15.
[26] Virtanen, P., Gommers, R., Oliphant, T. E., Haberland, M., Reddy, T., Cournapeau, D., Burovski, E., et al., 2020, "Scipy 1.0: Fundamental Algorithms for Scientific Computing in Python," Nat. Methods, **17**(3), pp. 261–272.
[27] Storn, R., and Price, K., 1997, "Differential Evolution: A Simple and Efficient Heuristic for Global Optimization Over Continuous Spaces," J. Global Optim., **11**(4), pp. 341–359.
[28] Forrester, A. I. J., Sóbester, A., and Keane, A. J., 2008, *Engineering Design Via Surrogate Modelling: A Practical Guide*, J. Wiley, Chichester West Sussex UK and Hoboken NJ.
[29] Rasmussen, C. E., 2006, *Gaussian Processes for Machine Learning* (Adaptive Computation and Machine Learning Series), MIT Press, Cambridge, MA.
[30] Buitinck, L., Louppe, G., Blondel, M., Pedregosa, F., Mueller, A., Grisel, O., Niculae, V., et al., 2013, "API Design for Machine Learning Software: Experiences From the Scikit-Learn Project," arXiv:1309.0238.
[31] Shields, M. D., and Zhang, J., 2016, "The Generalization of Latin Hypercube Sampling," Reliab. Eng. Syst. Saf., **148**, pp. 96–108.
[32] Afzal, A., Kim, K.-Y., and Seo, J.-W., 2017, "Effects of Latin Hypercube Sampling on Surrogate Modeling and Optimization," Int. J. Fluid Mach. Syst., **10**(3), pp. 240–253.
[33] McKay, M. D., Beckman, R. J., and Conover, W. J., 1979, "A Comparison of Three Methods for Selecting Values of Input Variables in the Analysis of Output From a Computer Code," Technometrics, **21**(2), p. 239.
[34] Huntington, D. E., and Lyrintzis, C. S., 1998, "Improvements to and Limitations of Latin Hypercube Sampling," Probab. Eng. Mech., **13**(4), pp. 245–253.
[35] Pronzato, L., and Müller, W. G., 2012, "Design of Computer Experiments: Space Filling and Beyond," Stat. Comput., **22**(3), pp. 681–701.
[36] Mishra, S. K., 2006, "Some New Test Functions for Global Optimization and Performance of Repulsive Particle Swarm Method," SSRN Electron. J., North-Eastern Hill University, India.
[37] Han, M., Huang, Q., Ouyang, L., and Zhao, X., 2023, "A Kriging-Based Active Learning Algorithm for Contour Estimation of Integrated Response With Noise Factors," Eng. Comput., **39**(2), pp. 1341–1362.
[38] Yang, F., Lin, C. D., and Ranjan, P., 2020, "Global Fitting of the Response Surface Via Estimating Multiple Contours of a Simulator," J. Stat. Theory Pract., **14**(9).
[39] Cortes, C., and Vapnik, V., 1995, "Support-Vector Networks," Mach. Learn., **20**(3), pp. 273–297.
[40] Filzmoser, P., and Nordhausen, K., 2021, "Robust Linear Regression for High–Dimensional Data: An Overview," WIREs Comput. Stat., **13**(4), p. e1524.